TSUNAMI LOADINGS ON STRUCTURES
REVIEW AND ANALYSIS

Harry Yeh[1], Andre R. Barbosa[2], Harrison Ko[3], and Jessica Cawley[4]

The 2011 Great East Japan Tsunami has altered our traditional concepts for estimating loadings on structures. Prior to this event, we generally understood that reinforced concrete structures – those often used for critical coastal facilities – could withstand tsunami actions. This is no longer the case. Many concrete buildings and coastal protective structures (seawalls, coastal dykes and the like) failed due to the 2011 Tsunami. In this paper, the existing design guidelines are reviewed. We point out that some of the force-estimation methods recommended in the guidelines are rational, while others are not. Then we introduce a methodology to evaluate building's global stability emphasizing the effect of buoyant force. Buoyancy reduces the net structural body force; thereby reducing the restoring forces to resist sliding and overturning failures. Buoyancy force is an upward pressure force under the building, which is caused by an increase of pore-water pressure in the soil by excess water weight on the ground surface; therefore it takes a finite time to build up. We demonstrate that the effect of buoyancy force depends on 1) duration and depth of tsunami inundation, and 2) burial depth of the building. We also note that if and when a building interior is flooded (due to breakaway walls or windows), the flooded water increases the effective body force (weight); hence producing a stabilizing effect. Example calculations are given to demonstrate the importance of the delayed action of buoyancy force and breakaway walls and windows.

Keywords: buoyancy force; global structural failures; tsunami loadings.

INTRODUCTION

In 2011, a magnitude Mw 9.0 earthquake struck the coast of Japan's Tohoku region causing catastrophic damage together with the loss of 15,889 lives and 2,597 people still missing as of November 10, 2014 (National Police Agency of Japan, 2014). To strive towards constructing tsunami resilient communities, research has focused on the development of life saving mitigation strategies, such as creating early warning systems and effective evacuation routes. High ground is the safest place to evacuate during a tsunami. However, when insufficient time and geographical conditions prevent evacuation to high ground, an alternative is to move to a high elevation by climbing up to the top floor of a sturdy building that withstands the tsunami loads. FEMA P-646 (2012) provides methodologies for estimating these loads and shows some examples of existing reinforced concrete buildings that were designated as tsunami vertical evacuation buildings in Japan. Reinforced concrete (RC) buildings offer a balance between strength and weight needed to withstand the tsunami loads. In 1994, Shuto dismissed the idea that well-engineered reinforced concrete buildings could fail due to tsunami loadings based on observations from previous tsunamis. Shuto reported the only exception was the total destruction of the Scotch Cap Lighthouse by the 1946 Aleutian tsunami; this exception was due perhaps to the fact that the lighthouse was located right at the shoreline (e.g. Yeh 2009). Prior to the 2011 Tsunami, a brief discussion from the Building Research Institute in Japan suggested that building overturning could be a possible failure mechanism (Okada et al. 2006). The 2011 Tsunami caused many RC buildings to overturn and dragged many meters from their original location with little internal structural damage. These devastating global failures were surprising to many engineers. These failures were attributed to higher-than-expected inundation depths, high flow velocities, soil scour, and buoyancy effects (Yeh et al. 2013).

To evaluate the capacity of a building to withstand failures, the required parameters are: tsunami inundation and flow characteristics at the building site, building shape, effect of building water-tightness, type and depth of foundation, and soil characteristics. The design formulae presented in FEMA P-646 (2012), Asakura et al (2002), and Fujima et al (2009) can be used to estimate tsunami-induced forces. However, these do not consider the effects of time varying buoyancy forces due to the fast nature of the tsunami inundation processes and the gradual pore-water pressure response in the foundation soil. Figure 1 illustrates a typical time series of the complex combination of tsunami forces. In this figure, a dashed line represents the capacity of the structure to sliding. Note that there is a decrease in capacity that can be attributed to the buoyancy force reducing the resistance of the structure to sliding and overturning. Here we demonstrate that time varying buoyancy forces play a significant role in the global failure of the RC buildings.

---

[1] School of Civil & Construction Engineering, Oregon State University, Corvallis, Oregon, 97331, USA
[2] School of Civil & Construction Engineering, Oregon State University, Corvallis, Oregon, 97331, USA
[3] School of Civil & Construction Engineering, Oregon State University, Corvallis, Oregon, 97331, USA
[4] School of Civil & Construction Engineering, Oregon State University, Corvallis, Oregon, 97331, USA

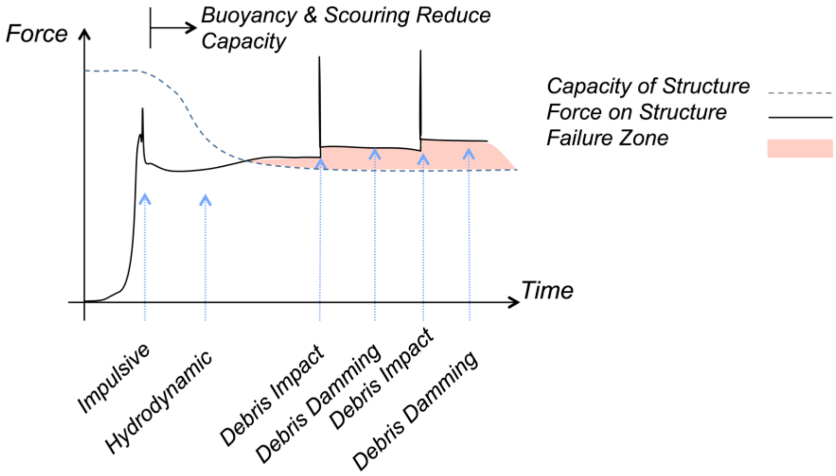

Figure 1. Typical time series of loading and capacity. An object is assumed inundated initially so that the impulsive force is greater than the subsequent hydrodynamic force, and the structural capacity decreases in time because of the gradual development of buoyancy force and scour action through the surrounding soils (to be discussed in detail later).

There are other factors that should be considered when estimating tsunami forces exerted on a building: for example, the presence of breakaway walls and windows that would provide substantial force alleviation (e.g. Dalrymple and Kriebel 2005; Lukkunaprasit et al. 2008; Yeh et al. 2013). The reduction in force can be attributed to two parts: (1) reduced frontal area of the building and (2) water entering the building. Since force is proportional to the area, the removed elements that "break away" reduce the force exerted on the structure. Nonetheless, it is important to recognize that in order to bypass flow's linear momentum, breakaway windows and walls must be "inline" with a flow path in and out of the building. Figure 2 shows two flat and narrow five-story apartment buildings that are oriented with the surface area facing the ocean. Despite their orientation and the fact that the inundation reached the top level, the buildings remained standing, most likely due to the force alleviation from the front-and-back well-aligned breakaway windows and doors creating many "punched holes" for the tsunami. In addition, it is noted that once the water inundates the structure it tends to act as a stabilizing force.

(a)

(b)

Figure 2. Example of breakaway windows in Rikuzen-Takata, Japan, due to the 2011 Tsunami. Most of the other surrounding buildings were wiped away. Note the breakaway windows and doors that might have reduced the tsunami loadings and enhanced the net body weight of the buildings.

The objective of this paper is to present current approaches for tsunami-force estimation on buildings and to describe estimates of the demand and capacity to global failure mechanisms, emphasizing the time-dependent effects of buoyancy. We provide a review of the present understanding of tsunami effects on buildings, including the classification of tsunami loadings on buildings, differentiating between the physical meaning and calculations of the hydrodynamic, hydrostatic, impulsive, debris impact and debris damming forces. We then present a comprehensive analysis for global failures of buildings by overturning and sliding.

OBSERVATIONS OF BUILDING TSUNAMI INDUCED DAMAGE

Building failures can be categorized into three classes. First, in the case of global stability failure, a building overturns and/or slides as a rigid body, typically with the lateral resisting system. The building itself suffers little or no structural damage. Overturning is defined as a rotation of a building about a point typically at the level of the foundation and sliding is defined as the global horizontal translation of a building. The failures shown in Fig. 3 are all in this class; it is noted that some were toppled in the landward direction and the others were in the seaward direction. In the second class, failure of one or more individual structural components (e.g. columns and beams) leads to the collapse of the building, typically caused by strong earthquake shaking. The third class is failure of the building foundation associated with soil instability and scour. Examples of buildings that slid and tilted observed in the recent reconnaissance surveys have been attributed to a combination of large horizontal forces and overturning with coinciding scouring. In this paper, we focus on the first class of failure modes – global stability failure; this failure mode had not been recognized as possible until recently (e.g. Yeh et al. 2013).

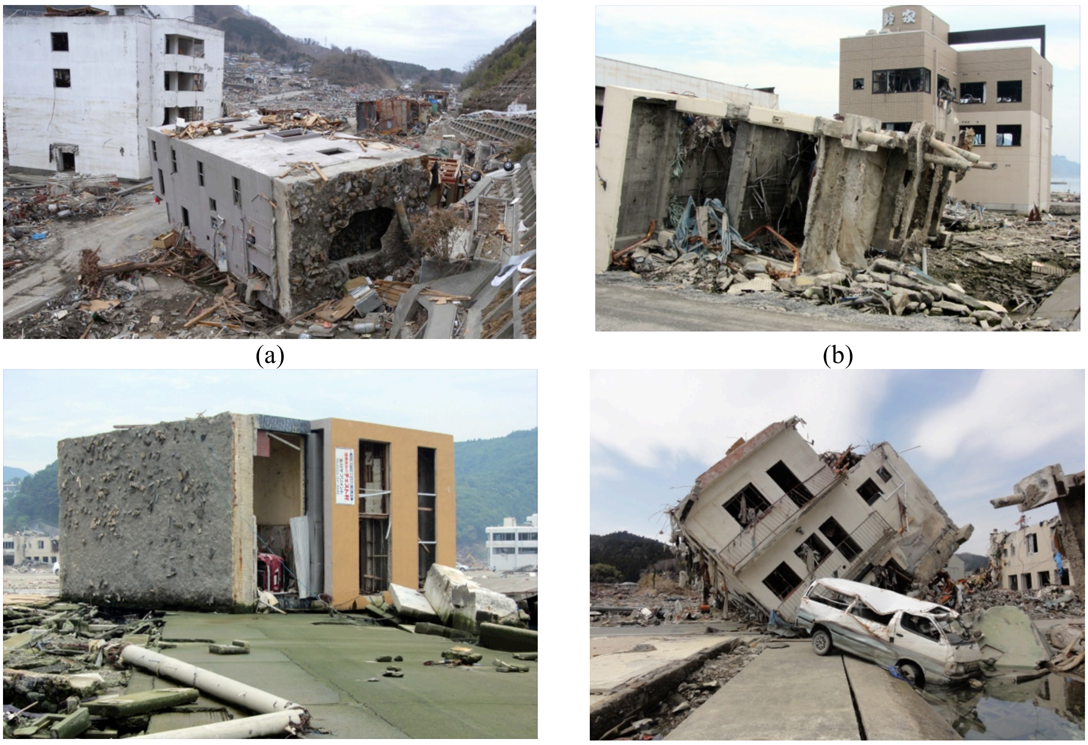

(a) (b) (c) (d)

Figure 3. The RC buildings in Onagawa were toppled by the 2011 Tsunami. Some had matt foundation and others had pile foundation. Photos (a) and (d) are by Koshimura.

DETERMINATION OF TSUNAMI INDUCED PARAMETERS

Tsunami Forces

Fundamentally, fluid forces $\vec{F}$ exerted on a noncompliant body are computed by

$$\vec{F} = \int_{\partial S} \tau_{ij}\, n_i \, ds \,, \tag{1}$$

where τ_{ij} is the stress tensor, n_i is the unit vector representing the direction normal to the surface ds, and ∂S is the net surface area of interest. The integrand in Eq. 1 can be split into two components: namely, the component normal to the surface ($i = j$), i.e. pressure, and the vector component tangent to the surface ($i \neq j$), i.e. shear stress. The two components are the basis of fluid loadings on a stationary rigid object.

For engineering estimates, tsunami forces are classified based on the flow conditions. For example, FEMA P-646 (2012) classifies the tsunami forces as (1) hydrodynamic forces induced by the steady flows, (2) hydrostatic forces under the quiescent flood states, (3) highly transient impulsive forces at the impact of the leading edge of the arriving water mass, (4) debris impact forces caused by the water-born missiles, and (5) debris damming forces. The classification is made for convenient engineering applications, but represents the complexity in the analysis of tsunami loadings that requires considering many possible conditions of tsunami actions. This factor is unique to the tsunami loading analysis.

The term *hydrodynamic force* is often used in tsunami literature (e.g. Dames & Moore, 1980; FEMA P646, 2012; Yeh, 2006, 2007). The hydrodynamic force is similar to, but not exactly the same as, the *drag force* used in the field of fluid dynamics. The term drag force is used for the force acting on a fully submerged body in a "steady" flow without the presence of air-water free surface. The drag force F_D is the component of the total force parallel to the ambient flow direction, and can be calculated by

$$F_D = \tfrac{1}{2} C_D A \rho U^2 , \tag{2}$$

where C_D is the drag coefficient, A is the projectional area of the body on the plane normal to the direction of ambient steady flow with the velocity U, and ρ is the fluid density. It is emphasized that the force given in Eq. 2 represents the drag force exerted on the submerged body as a whole. However, in tsunami literature, the form of Eq. 2 is also used for a water-surface-piercing object. Notably, theoretical justification for the use of Eq. 2 for gravity controlled free-surface flows is not rigorous; the drag coefficient C_D must be a function of gravity (i.e. Froude number) as well as object's characteristics (shape, surface roughness, orientation, etc.) and Reynolds number. Arnason et al. (2009) recognized this, and instead of the drag coefficient C_D, they introduced the term "the coefficient of resistance C_R" to distinguish the forces on a partially submerged object. Arnason et al. found that the form of Eq. 2 yielded good approximations to their laboratory experiments for a vertically erected square column, and the magnitude of C_R is comparable to C_D; i.e., $C_R \approx 2$ for a square column. It is anticipated that for a body that is not excessively elongated in the flow direction, the dominant force is the 'form drag', which is caused by the pressure difference in front and back of the body. In summary, Eq. 2, which is often used to calculate tsunami's hydrodynamic force, is well founded by the hydrodynamics and can be justified for the use to evaluate the net fluid force on a body in a quasi-steady flow.

The *hydrostatic force* is a force under the static condition in which the pressure force balances with the gravitational body force, namely:

$$\frac{\partial p}{\partial z} = -\rho g , \tag{3}$$

where p is the pressure, and the coordinate z points upward. The hydrostatic condition exists in the absence of inertial and viscous forces. The hydrostatic force can be calculated by integrating the pressure field obtained in Eq. 3 over the surface of interest. The hydrostatic force is often calculated for the force acting on one side of a building's component surface, e.g. walls and windows. Note that, when a fluid is in motion around a body, the hydrostatic condition no longer exists. Instead, vertical flow accelerations can form in the wake on the leeside of the body, and horseshoe vortices can form around the front face. Nonetheless, the deviation caused by such flow accelerations is usually small in comparison with the hydrostatic component.

The integration of the vertical component of the hydrostatic pressure produces a net upward force, which is called the *buoyancy force*. The buoyancy force is equivalent to the fluid weight displaced by a body: i.e. Archimedes' principle (e.g. Lamb 1960). Yeh et al (2013) estimated that when the building shown in Fig. 3a was fully submerged and if it were watertight, then it could have failed solely by the buoyancy force without any water flow. It is emphasized that Yeh et al. (2013) blindly followed Archimedes' principle and calculated the buoyancy force without consideration of the building embedment in the soil. To conceptualize the importance of the buoyant force for tsunami problems, consider a body that is partially buried in the ground, such as a building with a basement. To establish tsunami-induced upward pressure, the excess pore-water pressure in the soil must increase during tsunami inundation: the response of excess pore-water pressure is however not an instantaneous reaction to the water-surface variations. This fact has not been recognized in the previous design guidelines such as FEMA P-646 (2012) and Dames & Moore (1980).

To consider the pore-water pressure gradients (i.e. buoyancy forces), Biot's (1941) poroelasticity theory could be used; however, Biot's equations require physical parameters that are hard to measure or estimate. Instead, we suggest a simpler equation, Terzaghi's (1956) consolidation equation to predict excess pore-water pressure dissipation:

$$\frac{\partial p_e}{\partial t} = c_v \nabla^2 p_e , \tag{4}$$

where p_e is the excess pore pressure; i.e., $p_e(t) = p(t) + \rho g z$. The coefficient of consolidation, c_v, can be expressed as (e.g., Holtz and Kovacs 1981)

$$c_v = \frac{k}{\rho g} \frac{1+e_0}{a_v} , \tag{5}$$

where k is the hydraulic conductivity in Darcy's Law, e_0 is the void ratio when no external stress is applied, and a_v is the coefficient of compressibility. The values of k and a_v can change during the tsunami inundation due to deformation of the soil fabric, which indicates that c_v is a function of p_e. Consequently, Eq. 4 is nonlinear for finite value of ∇p_e. Considering that the nonlinearity is negligible, we assume a constant value of c_v for a given soil medium. Values of c_v for sandy soils, which are typically found in coastal areas, are seldom experimentally measured, because the excess pore-water pressure usually dissipates 'quickly' in sandy soils. For this reason, tsunami inundation problems have not been fully examined in the field of geotechnical engineering. Yeh et al. (2004) used an apparatus that controlled the rapid pressure relief on the soil surface so that the values of c_v could be determined by Eq. 4 with direct measurements of the pore pressures. Their experimental data show that the average value of c_v for the sand they used (d_{50} = 0.26 mm, e_0 = 0.57 ~ 0.77) is 750 cm^2/s, ranging from 400 to 1200 cm^2/s.

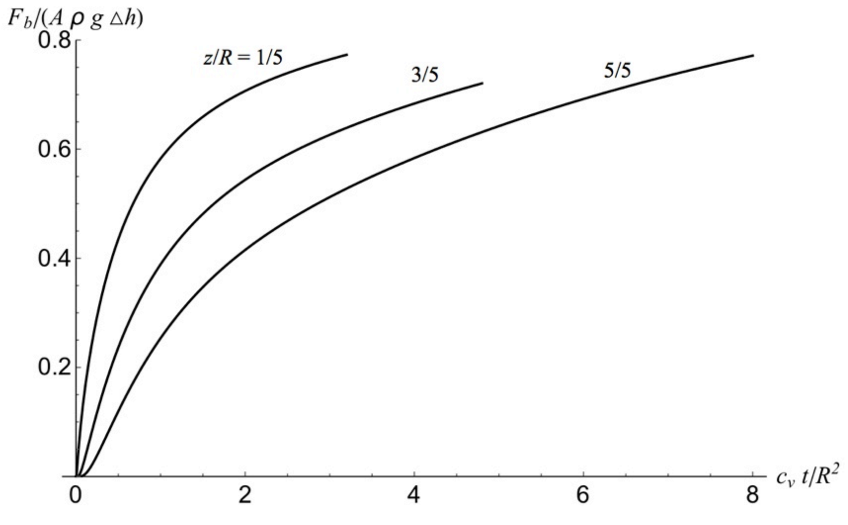

Figure 4. Temporal development of buoyancy forces under a cylindrical shaped building with radius 5 m. The cylindrical building is subjected to an instantaneous flood with depth *h*. Time *t* is normalized with the consolidation coefficient C_v and the radius R; the buoyancy force is normalized by the equilibrium value with the flood level Δh

Figure 4 shows the temporal variations of buoyancy forces under a vertically erected cylindrical building computed by Eq. 4. The excess buoyancy force is induced by an instantaneous inundation load

Δh at t = 0s and the inundation level being kept constant afterward. The cylindrical shaped building with a radius R is used since it allows us to compute the buoyancy effect on a 3D axisymmetric building with the 2D governing equation with the cylindrical coordinates:

$$\frac{\partial p_e}{\partial t} = c_v \left(\frac{1}{r} \frac{\partial}{\partial r} \left(r \frac{\partial p_e}{\partial r} \right) + \frac{\partial^2 p_e}{\partial z^2} \right), \tag{6}$$

where r and z are is the radial and vertical coordinates, respectively. The results in Fig. 4 for the different embedment depths z show that the buoyancy force establishes more quickly for the shallower embedment depths z/R. This suggests that buildings with basements should be more resilient to tsunami loading than buildings without basements, because the buoyancy force reduces the net building body force (weight). The results in Fig. 4 also show that for a given relative embedment z/R, the buoyancy force is a monotonically increasing function of the parameter $c_v\, t/R^2$ approaching its equilibrium state. This indicates that the more permeable the soils and the smaller the building base area, the faster the establishment of buoyancy force results. For a building with R = 5 m and z = 1 m in sandy soils with 400 cm^2/s < c_v < 1200 cm^2/s, 50% of the equilibrium buoyancy force (at $t \to \infty$) will be reached in 415 ~ 138 s, respectively. Evidently, such a time scale is comparable to a typical tsunami-inundation time scale, indicating that inclusion of the delayed buoyancy effect is important for the analysis.

The *impulsive force* is caused by the impingement of a leading edge of initial surging water onto a structure. The impulsive force acts only on the front side of the structure. Because the surge flow (and thus impulsive force) is highly transient, it is important to consider ductility of the impacted structure. Presently, there is no established and rational method available to predict the force. As a related problem, Cumberbatch (1960) presented a similarity solution of the initial impact of a fluid "wedge" onto a rigid wall. To estimate the impulsive force, Cross (1967) proposed to add the hydrostatic-pressure force to Cumberbatch's similarity solution. Arithmetically adding the hydrostatic force to Cumberbatch's analysis cannot be supported for this nonlinear flow action. In addition, estimating the water depth for a highly transient, boundary dominated flow at the leading edge of surging water is ambiguous. Other derivations from the original Cross's (1967) approach (e.g. Paczkowski et al. 2011) face the similar problems; i.e., justifying the rationality of the approach and identifying unambiguous model parameters are both problematic. Based on the laboratory study of Ramsden (1993), Yeh (2007) pointed out that the impulsive forces of surges over dry-land are smaller than the subsequent quasi-steady hydrodynamic forces: he postulated that the relatively small water-surface slope of the leading edge of the surge when it advances on a dry bed is the primary reason. In the case of a broken wave propagating onto a shallow quiescent-water depth (i.e. the formation of a bore), the front surface of the bore becomes steeper. Note that the bore flow condition differs from the surge flow condition: a surge advances on a dry bed. Based on two independent laboratory studies of Ramsden (1993) and Arnason (2005), the upper limit of the impulsive force caused by a bore is approximately 150% of the subsequent maximum hydrodynamic force (Eq. 2) in a quasi-steady flow. It is emphasized that this finding is empirical based on the two small-scale laboratory studies.

Debris impact forces are difficult to estimate. Several engineering attempts have been made previously, and they are summarized in Appendix D of FEMA P-646 (2012). Unlike other forces, debris impact forces occur locally at the point of contact when the debris is smaller than the building. Theoretically, debris impact forces can be evaluated with the impulse-momentum principle; i.e. the impulse of the resultant force acting for an infinitesimal time is equal to the change in linear momentum. Nonetheless, application of the theory in practice is difficult due primarily to uncertainty in the determination of impact time duration. Because of the difficulty, FEMA P-646 (2012) suggests to use a simplified model of the single-degree-of-freedom oscillator, instead of the impulse-momentum principle. The oscillator model is a linear model involving several parameters that need to be determined relying on 'engineering judgments'. In spite of such engineering struggles, its basic form $F \propto u\, m^{1/2}$ resembles the empirical formula derived from the extensive laboratory experiments conducted by Matsutomi (1999), which can be considered as a weak justification for this approach.

The *debris damming forces* are due to the jamming effect of debris on a structure, which increases the hydrodynamic forces by increasing the surface area exposed to the flow. This force follows after the initial impact force of the debris: see for example see Fig. 1. FEMA P-646 (2012) defines this force using Eq. 2, but replacing the width of the structure with the width of the jammed debris, thus increasing the force.

TSUNAMI INDUCED GLOBAL STRUCTURAL FAILURE ASSESSMENT

Formulation

We focus on the global failure of buildings, specifically those caused by gradually varying quasi-steady tsunami inundation. The only tsunami-induced forces analyzed here are hydrodynamic and buoyancy forces: transient impulsive and debris impact forces are not considered. It is important to recognize that the effective gravitational body force is the one that stabilizes a structure, whereas lateral external forces cause the system to become unstable and lead to failures. The effective body force W_e consists of the weight of building W_b, the weight of flooded water inside the building W_w, and the negatively acting buoyancy force F_B on the underneath of the foundation, namely,

$$W_e(t) = W_b + W_W(t) - F_B(t), \tag{7}$$

where the buoyancy force is evaluated using Eq. 4. The flooded water inside the building and the buoyancy force are time variant affected by the inundation time history. Figure 5 shows the general model considered for assessing the global stability.

Two stability conditions are considered: (i) incipient sliding and (ii) incipient overturning. Incipient sliding occurs when the sum of horizontal forces F_H is greater than zero,:

$$\sum F_H(t) = F_X(t) - R_X(t), \tag{8}$$

where $F_X(t)$ is the sum of the external forces acting on the building (in the present case, this is the hydrodynamic force $F_D(t)$), and $R_X(t)$ is the resisting force:

$$R_X(t) = \mu W_e(t) - (F_A - F_P), \tag{9}$$

where F_A and F_P are the active and passive soil pressure forces, respectively, $\mu = \tan \phi$ is the friction coefficient (ϕ is the friction angle). Incipient overturning results when the sum of clockwise moments about a reference point (point O in Fig. 5) becomes greater than zero:

$$\sum M_0(t) = \left(\tfrac{1}{2}h(t) + h_f\right)F_X(t) + \tfrac{1}{3}h_f(F_A - F_P) - \tfrac{1}{2}aW_e(t), \tag{10}$$

where a is the dimension of the building in the flow direction, and h_f is the depth of embedment.

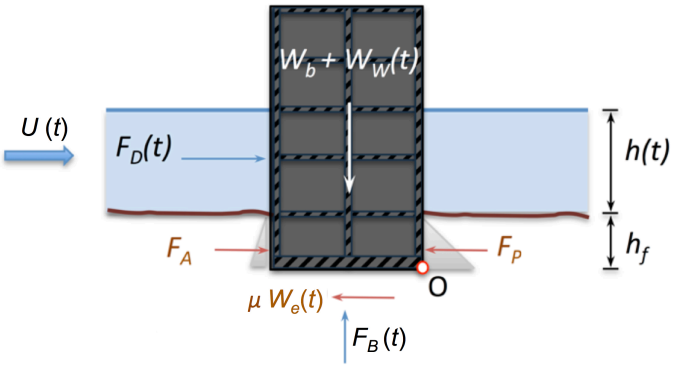

Figure 5. Free body diagram used in global stability analysis. F_D is the external hydrodynamic force; W_b is the dry weight of the building; w_w is the weight of the flooded water inside of the building; F_B is the buoyancy force; F_A and F_P are active and passive soil pressure forces, respectively; μ is the friction coefficient. The moment is computed about the foundation base point "O".

Application Example

To demonstrate the application of the formulation, we analyze the global stability for a four-story RC (reinforced-concrete) building, focusing on estimating the onset of overturning and sliding. This building is hypothetically located in Onagawa, and is imposed to the flood-depth and velocity time histories of the 2011 Tsunami reported by Koshimura and Hayashi (2012). Because the rise and fall of the water level inundation was relatively gradual, we consider the applied forces to be the hydrodynamic forces, buoyant forces, and additional retained water loading due to flooding in the building. The building is assumed to be 8.9 m wide, 8.9 m long, and 16 m high above ground level, which is similar to the one shown in Fig. 3a, and the tsunami flows are headed square to the building face. To estimate the building weight, we assume 10% of the total volume of the building is made of reinforced concrete (slabs, walls, columns, etc.) with the density ρ_c = 2,400 kg/m^3. Density of water is assumed ρ_w = 1,100 kg/m^3 accounting for the sediment laden flows. Saturated soil density is taken γ_s = 20 kN/m^3 with the friction angle ϕ = 30°, and the water table is assumed near the ground level. Equation 6 for a cylindrically shaped building with the radius R = 5 m is used to estimate the buoyancy forces of the 8.9 × 8.9 m square building: the error is expected to be small because of the equivalent base area. A parametric study is performed considering: (i) 3 levels for overburden (foundation) depth (z = 1, 3, and 5 m); (ii) 3 levels for the soil consolidation coefficient (c_v = 100, 400, and 700 cm^2/s); and, (iii) 2 levels for building water tightness (full water-tight and partially flooded assuming 80% of the volume being flooded).

Figures 6a and 6b show the time histories of flow velocity and inundation depth, respectively. While the depth time series is taken directly from the data given by Koshimura and Hayashi (2012), the flow velocities are estimated using parabolic-curve fitting based on the two maximum-speed data points reported by Koshimura and Hayashi: 6.3 m/s during the runup and 7.5 m/s during the drawdown process. Figure 7a shows the hydrodynamic force F_D (= F_X) computed using Eq. 2. Figure 7b illustrates the hydrodynamic moment about a point on the ground surface, given by:

$$M_0(t) = \tfrac{1}{2} h(t) F_X(t). \tag{11}$$

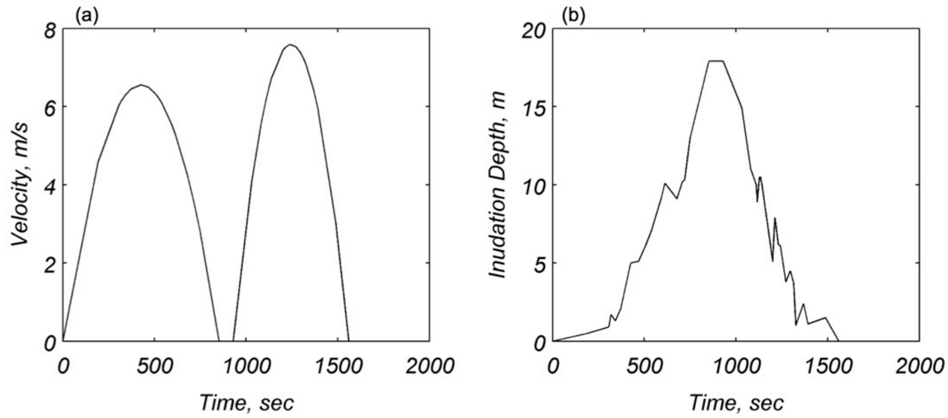

Figure 6. Tsunami flow characteristics obtained from the video footage for the town of Onagawa, Japan, during the 2011 Tsunami. (a) flow velocity, and (b) inundation depth.

It can be seen from Fig. 7 that the peak hydrodynamic force does not need to occur at the same instant as the peak moment. The parameter needed to compute the hydrodynamic moment is the square of the product of flow velocity and depth (h U)^2, whereas the parameter needed to compute the hydrodynamic force is h U^2.

Figure 8a shows the buoyancy-force variations for three different overburden depths z = 1, 3, and 5 m with c_v = 100 cm^2/s, while Fig. 8b shows the variations of the buoyancy force for c_v = 100, 400, and 700 cm^2/s with z = 1 m. It can be seen that for the deeper overburden depth, the peak buoyant force becomes smaller and takes longer to develop. As the soil consolidation coefficient c_v increases, the buoyant force develops faster and reaches the greater peak value. Figure 8 clearly demonstrates that the time history of tsunami inundation is crucial to the determination of the buoyancy force.

Figure 9a shows the applied horizontal tsunami forces F_X and the resisting R_X force normalized by the net weight of the watertight building prior to the tsunami arrival, i.e. $W_{b,0}^{net} = W_e(t \le 0)$ in Eq. 7. The results are shown for the constant foundation depth (z = 1 m) and three different values of the consolidation coefficient. While the applied forces F_X are the same, the resistance varies with the consolidation coefficient because the buoyancy force affects its stability. As the buoyancy force increases faster for the case of larger c_v, the reduction of the resisting force is also greater, leading to an unstable state earlier on. Note that the condition of F_X > R_X is the indicator of sliding failure (see Eq. 8).

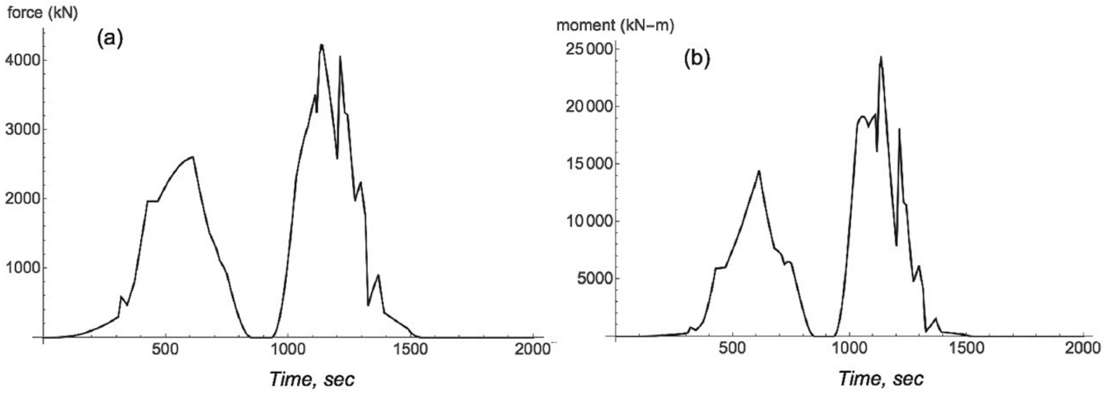

Figure 7. Tsunami force and moment time-histories for tsunami inundation shown in Fig. 6: (a) hydrodynamic force, and (b) hydrodynamic moments for a building with the foundation 1m deep.

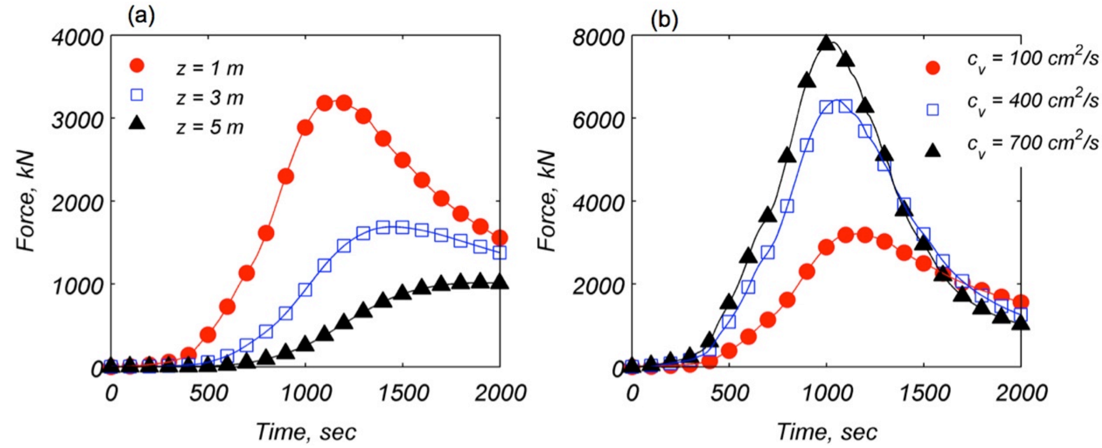

Figure 8. Effect of overburden depth and consolidation coefficient on buoyancy force time-histories for tsunami inundation shown in Fig. 6: (a) z = 1, 3, and 5 m with c_v = 100 cm^2/s and (b) c_v = 100, 400, and 700 cm^2/s with z = 1 m.

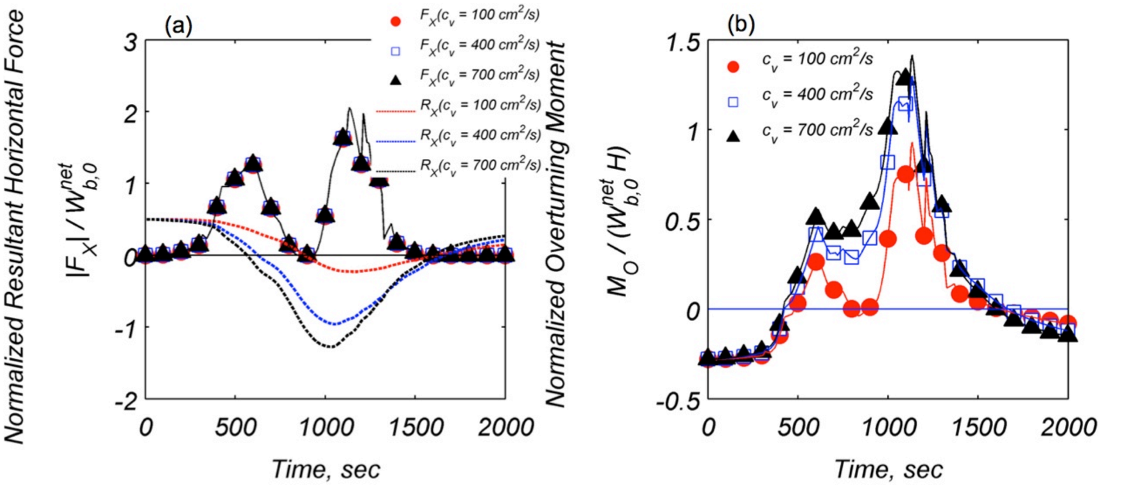

Figure 9. Effect of consolidation coefficient on the stability of the watertight building for tsunami inundation shown in Fig. 6: (a) normalized horizontal applied forces and resisting forces, and (b) normalized overturning moments.

In Fig. 9b, the value of overturning moment greater than zero ($M_0 > 0$, see Eq. 10) corresponds to instability by overturning around the base of the building. Figure 9 shows that the smaller the consolidation coefficient the more stable the building, highlighting the effect of delay in the buoyance-force development. Nonetheless, all of the cases result in both sliding and rotational failures. The tsunami drawdown causes more severe condition to the building than the runup process, partly because of the delayed development of buoyancy force, and the buoyancy force tends to make a building unstable.

We anticipate that the effect of breakaway walls and windows has a great influence in building stability. This is demonstrated in Fig. 10: the building is now assumed to be 80% floodable proportional to the inundation depth. The imposed flooded condition leads to a system that is more stable than the watertight building. In fact, Fig. 10 shows that regardless of the three selected foundation soil types (c_v = 100, 400, and 700 cm^2/s), the building does not fail by sliding nor by rotation during the runup process; it does, however, fail during the drawdown phase. This substantial increase in stability is attributed to the fact that flooding the building increases the net body force (weight). Furthermore, the breakaway walls and windows can lead to a reduction of the horizontal forces when such walls and windows are aligned in the flow direction so that the flow momentum can be bypassed through the building, although this effect is not modeled here.

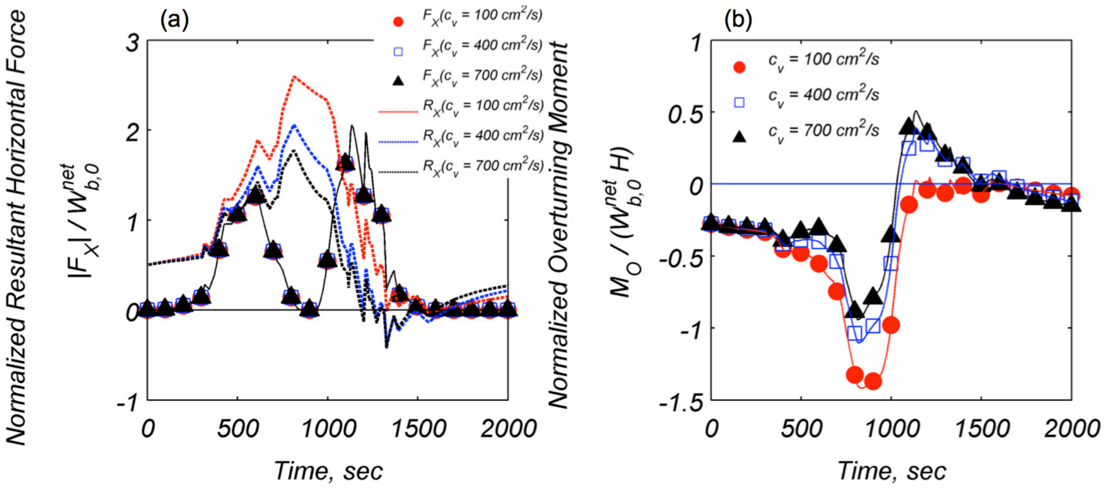

Figure 10. Effect of consolidation coefficient on the stability of the 80% flooded building for tsunami inundation shown in Fig. 6: (a) normalized horizontal applied forces and resisting forces, and (b) normalized overturning moments.

Figure 11 and 12 show the results in which the c_v is held constant at 100 m^2/s and the foundation depths are varied: z = 1, 3, and 5 m. Figure 11 shows that the increase of the foundation depth increases the propensity for instability mainly due to the reduction of the initial net weight of the building: in other words, the net building weight with the deeper foundation depth is smaller due to the initial buoyancy force prior to the tsunami arrival. This is the reason why the normalized resultant horizontal forces appear as the different curves depending on the three foundation depths, even though the actual external forces are identical. Figure 11 implies that the deeper the foundation becomes the faster the failure. It is emphasized that this trend results from the difference in initial instability prior to the tsunami attack. In fact, with the equivalent initial stability (the same initial buoyancy forces), the building with the deeper the foundation would perform better for the same tsunami loadings.

During tsunami inundation, it can be seen that the reduction of the resistance R_X for the deeper foundation is more gradual. This is highlighted in Fig. 11, where the normalized resistance of the building with the deeper foundation is notably greater than the building with the shallower foundation.

Figure 12 shows the effect of flooded water (80% of the inundation depth) inside of the building. As seen in Fig. 11, both external horizontal forces and moments are normalized by the 'initial' net weight of the building, which varies depending on the foundation depth z. Nonetheless, the effect of breakaway walls and windows is evidently substantial: the imposed flooded condition leads to a system far more stable than the watertight building. In fact, Fig. 12 indicates that except for a very short duration in the case of z = 5m, the tsunami cannot cause either sliding or rotational building failure. It is important to point out that the resisting forces are significantly greater for the deeper foundation depth. During the drawdown phase, all of the cases could fail both by sliding and rotation, although the failure duration is very short.

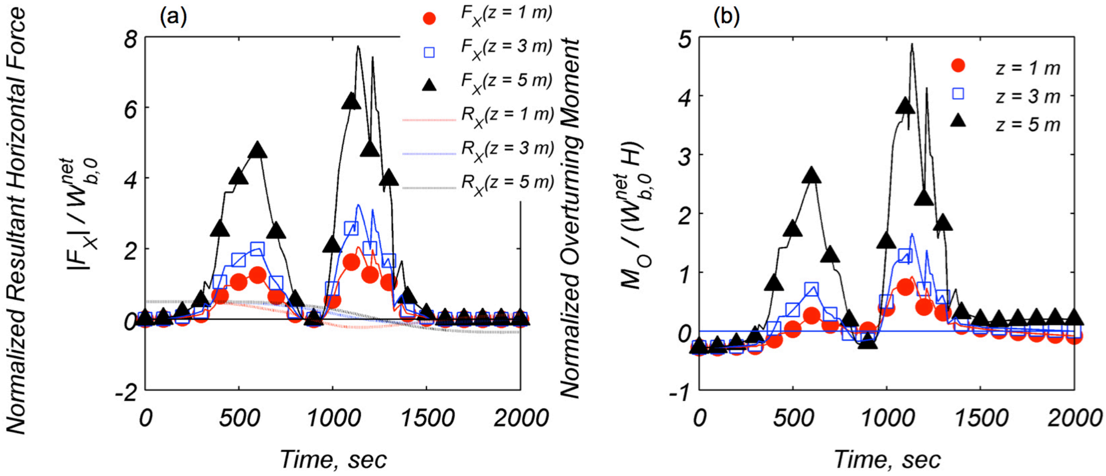

Figure 11. Effect of overburden depth on the stability of the watertight building for tsunami inundation shown in Fig. 6: (a) normalized horizontal applied forces and resisting forces, and (b) normalized overturning moments.

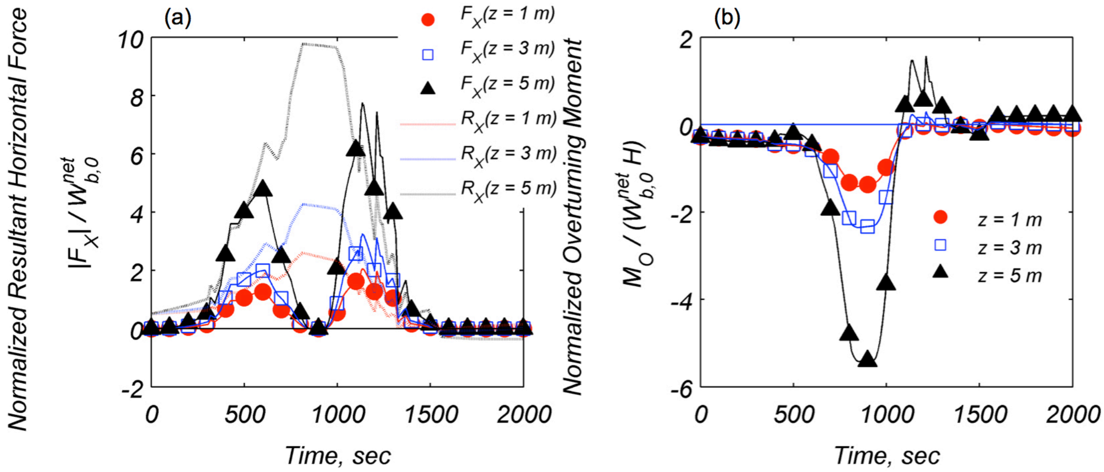

Figure 12. Effect of overburden depth on the stability of the 80% flooded building: (a) normalized horizontal applied forces and resisting forces, and (b) normalized overturning moments.

CONCLUSION

The 2011 Tsunami has altered our traditional understanding of RC buildings that were thought to be invulnerable to tsunami loadings. Many RC buildings failed due to overturning and sliding. Unlike other natural hazards, we need to consider many scenarios for tsunami loadings. It is discussed that adapting the concept of drag force in fluid mechanics, the hydrodynamic force for a partially submerged building in quasi-steady flows is well founded and supported by laboratory experiments. The hydrostatic force is for the "static" condition acting on a surface. Applications of buoyancy force to the buildings must consider the effects of soil and foundation, because the buoyancy force acts on the bottom of the building. We point out that existing methods to estimate the impulsive forces and the debris impact forces are ambiguous and more or less rely on engineering "judgment."

The building-failure patterns observed from the 2011 Tsunami were not unique: some failed during runup (buildings found inland) and others failed during drawdown (building pushed seaward).

This implies that the external flow force alone may not control the building failures, but building stabilities weakened by the buoyancy force may play a role in the failures.

To estimate the overturning moment, a necessary flow parameter is the square of the product of inundation depth and flow speed $(hU)^2$, whereas it is well known that the parameter – the specific force hU^2 – is needed to evaluate the horizontal hydrodynamic forces. The maxima of those parameters should be added to the list of parameters to extract from the numerical hydrodynamic simulations for structural analysis.

Using the tsunami inundation data of the 2011 Tsunami in the town of Onagawa, we demonstrated that the buoyancy-force calculations are essential to evaluate global building failures. The development of buoyancy force follows a process of diffusion, and therefore, does not respond instantaneously to the inundation level. Consequently, the development of buoyancy force depends on the foundation embedment and the consolidation coefficient that is closely related to soil's permeability (Eq. 5). The response time is slower for the deeper foundation and the smaller the consolidation coefficient. Therefore, the excess buoyancy forces could be mitigated for the buildings with deeper foundations (i.e. with basements) and wider impermeable fringes placed around the buildings. Furthermore, the buildings could be more stabilized when the interior is flooded due to breakaway walls, windows, and doors. This is because the flooded water acts as the extra body force to resist from the failure. Common understanding of the breakaway walls and windows is the reduction of surface areas exerted by the flow forces. However, it is emphasized that this is effective only when the breakaway openings of the buildings from the front and the back are aligned with the tsunami flow direction so that the flow momentum can be effectively bypassed through the building.

ACKNOWLEDGMENTS

This work was supported by the Oregon State University Edwards Endowment and the Pacific Earthquake Engineering Research Center at the University of California, Berkeley. A personal invitation to ICCE 2024, Soul, Korea, made by Professor Dosam Kim of Korea Maritime and Ocean University is acknowledged.

REFERENCES

Arnason, H. 2005. *Interactions between an Incident Bore and a Free-Standing Coastal Structure*, Ph.D. Thesis, University of Washington, Seattle, 172 pp.

Arnason H, C. Petroff, H. Yeh. 2009. Tsunami bore impingement onto a vertical column. *J. Disaster Research*, 4 (6), 391-403.

Asakura, R., K. Iwase, T. Ikeya, M. Takao, T. Kaneto, N. Fujii, M., and Ohmori. 2002. The tsunami wave force acting on land structures, *Proceedings of the 28th International Conference on Coastal Engineering*. ASCE, 1191-1202.

Biot, M.A. 1941. General theory of three-dimensional consolidation. *J. Appl. Phys*. 12: 155-164.

Cross, R.H. 1967. Tsunami surge forces, *Journal of Waterways and Harbor Division*, ASCE 93:4, 201-231.

Cumberbatch, E. 1960. The impact of a water wedge on a wall, *Journal of Fluid Mechanics* 7, 353–374.

Dalrymple R A, D.L.Kriebel. 2005. Lessons in engineering from the tsunami in Thailand. *The Bridge*, 35(2): 4-13.

Dames & Moore. (1980). *Design and Construction Standards for Residential Construction in Tsunami-Prone Areas in Hawaii*. Washington, D.C.: Prepared for the Federal Emergency Management Agency.

FEMA P-646. 2012. *Guidelines for Design of Structures for Vertical Evacuation from Tsunamis* (2nd Ed.), Federal Emergency Management Agency, Washington, D.C., 174 pp

Fujima, K., F. Achmad, Y. Shigihara, and N. Mizutani. 2009. Estimation of tsunami force acting on rectangular structures. *Journal of Disaster Research*, *4*(6), 404–409.

Holtz, R.D. and W.D. Kovacs. 1981. *An Introduction to Geotechnical Engineering*. Prentice Hall. New Jersey, 733pp.

Koshimura, S. and S. Hayashi. 2012. Tsunami flow measurement using the video recorded during the 2011 Tohoku tsunami attack. *Geoscience and Remote Sensing Symposium (IGARSS)*, 2012 IEEE International, 6693-6696.

Lamb H, 1960. *Statics*. Cambridge University Press, 361pp.

Lukkunaprasit, P., C. Chinnarasri, A. Ruangrassamee, and S. Weesakul. 2008. Experimental Investigation of Tsunami Wave Forces on Buildings with Openings. *Solutions to Coastal Disasters Conference*, COPRI, ASCE.

Matsutomi, H. 1999. A practical formula for estimating impulsive force due to driftwoods and variation features of the impulsive force. *Proceedings of the Japan Society of Civil Engineers*, 621, 111-127 (in Japanese).

National Police Agency of Japan, 2014: http://www.npa.go.jp/archive/keibi/biki/higaijokyo.pdf

Okada, T., T. Sugano, T. Ishihara, S. Takai, and T. Tateno. 2006. *Tsunami Loads and Structural Design of Tsunami Refugee Buildings.* Building Technology Research Institute.

Ramsden, J.D. 1993. *Tsunamis: Forces on a vertical wall caused by long waves, bores, and surges on a dry bed*. Report No. KH-R-54, W.M. Keck Laboratory, California Institute of Technology, Pasadena, Calif., 251 pp.

Shuto, N. 1994. *Building damages due to the Hokkaido Nansei-Oki Earthquake and Tsunami*, Tsunami Engineering Technical Report No. 11, Tohoku University, 11 – 28. (in Japanese)

Terzaghi, K. 1956. *Varieties of submarine slope failures*. Harvard Soil Mechanics Series 52, Cambridge MA.

Yeh, H. 2006. Maximum fluid forces in the tsunami runup zone, *Journal of Waterway, Port, Coastal, and Ocean Engineering*, ASCE, 132, 496-500.

Yeh, H. 2007. Design tsunami forces for onshore structures, *J. Disaster Research*, 2, 531-536.

Yeh, H. 2009. Tsunami Impacts on Coastlines. In: *The Sea, Vol. 15* (Ed: E.N. Bernard and A.R. Robinson), Harvard University Press. 333-369.

Yeh, H., S. Sato, and Y. Tajima. 2013. The 11 March 2011 East Japan Earthquake and Tsunami: Tsunami Effects on Coastal Infrastructure and Buildings. *Pure Appl. Geophys.,* 170, 1019-1031.

Yeh, H., S. Tonkin, E. Heller, P. Arduino, F. Kato, and S. Sato. 2004. Mechanisms of scour induced by tsunami runup. *Proceedings of the 2nd International Conference on Scour and Erosion*, Singapore, 2, 464-471.